HHS Public Access

Author manuscript

J Am Chem Soc. Author manuscript; available in PMC 2024 March 08.

Published in final edited form as:

J Am Chem Soc. 2022 December 28; 144(51): 23543–23550. doi:10.1021/jacs.2c10558.

Human EXOG Possesses Strong AP Hydrolysis Activity: Implication on Mitochondrial DNA Base Excision Repair

Michal R. Szymanski,
Department of Pharmacology and Toxicology and Sealy Center for Structural Biology, University of Texas Medical Branch, Galveston, Texas 77555, United States; Intercollegiate Faculty of Biotechnology, University of Gdansk and Medical University of Gdansk, 80-307 Gdansk, Poland

Anna Karlowicz,
Intercollegiate Faculty of Biotechnology, University of Gdansk and Medical University of Gdansk, 80-307 Gdansk, Poland

Geoffrey K. Herrmann,
Department of Pharmacology and Toxicology and Sealy Center for Structural Biology, University of Texas Medical Branch, Galveston, Texas 77555, United States

Yana Cen,
Department of Medicinal Chemistry, School of Pharmacy, Virginia Commonwealth University, Richmond, Virginia 23298, United States

Y. Whitney Yin
Department of Pharmacology and Toxicology, Sealy Center for Structural Biology, and Department of Biochemistry and Molecular Biology, University of Texas Medical Branch, Galveston, Texas 77555, United States

Abstract

Most oxidative damage on mitochondrial DNA is corrected by the base excision repair (BER) pathway. However, the enzyme that catalyzes the rate-limiting reaction—deoxyribose phosphate (dRP) removal—in the multienzymatic reaction pathway has not been completely determined in mitochondria. Also unclear is how a logical order of enzymatic reactions is ensured. Here, we present structural and enzymatic studies showing that human mitochondrial EXOG (hEXOG) exhibits strong 5′-dRP removal ability. We show that, unlike the canonical dRP lyases that act on a single substrate, hEXOG functions on a variety of abasic sites, including 5′-dRP, its oxidized

Corresponding Authors: **Michal R. Szymanski** – *Department of Pharmacology and Toxicology and Sealy Center for Structural Biology, University of Texas Medical Branch, Galveston, Texas 77555, United States; Intercollegiate Faculty of Biotechnology, University of Gdansk and Medical University of Gdansk, 80-307 Gdansk, Poland;* michal.szymanski@ug.edu.pl; **Yana Cen** – *Department of Medicinal Chemistry, School of Pharmacy, Virginia Commonwealth University, Richmond, Virginia 23298, United States;* ceny2@vcu.edu; **Y. Whitney Yin** – *Department of Pharmacology and Toxicology, Sealy Center for Structural Biology, and Department of Biochemistry and Molecular Biology, University of Texas Medical Branch, Galveston, Texas 77555, United States;* ywyin@utmb.edu.

Supporting Information

The Supporting Information is available free of charge at https://pubs.acs.org/doi/10.1021/jacs.2c10558.
Materials and methods, supplementary results, and Figures S1–S7 (PDF)

Complete contact information is available at: https://pubs.acs.org/10.1021/jacs.2c10558

The authors declare no competing financial interest.

product deoxyribonolactone (dL), and the stable synthetic analogue tetrahydrofuran (THF). We determined crystal structures of hEXOG complexed with a THF-containing DNA and with a partial gapped DNA to 2.9 and 2.1 Å resolutions, respectively. The structures illustrate that hEXOG uses a controlled 5′-exonuclease activity to cleave the third phosphodiester bond away from the 5′-abasic site. This study provides a structural basis for hEXOG's broad spectrum of substrates. Further, we show that hEXOG can set the order of BER reactions by generating an ideal substrate for the subsequent reaction in BER and inhibit off-pathway reactions.

Graphical Abstract

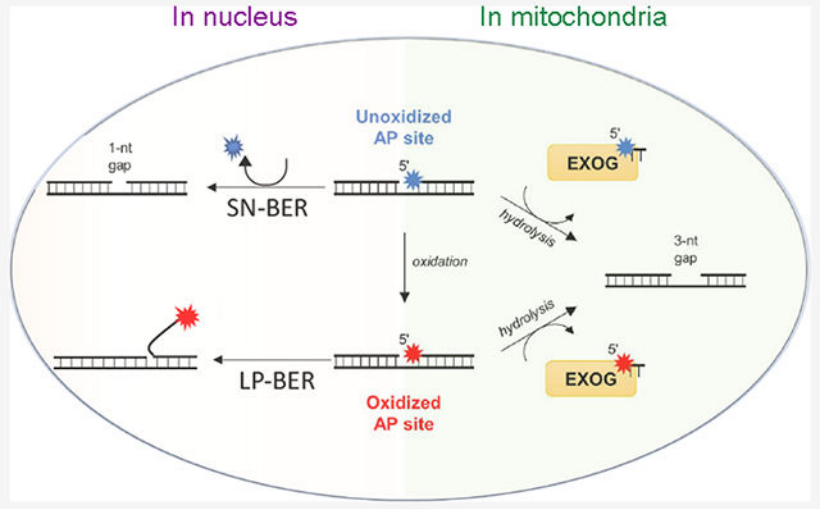

INTRODUCTION

Mitochondrial DNA suffers more oxidative damage than nuclear DNA due to a higher concentration of endogenous reactive oxygen species.[1] Oxidative DNA damage is resolved mostly by base excision repair (BER), a multienzymatic reaction pathway.

BER consists of five basic steps (Scheme 1): lesion nucleobase removal by a glycosylase, cleavage of the DNA backbone by an AP endonuclease yielding a 5′-deoxyribose phosphate abasic site (5′-dRP or AP site) in the nicked DNA, removal of the AP site generating a gap in the DNA, gap-filling synthesis, and ligation to restore the integrity of the DNA. In mitochondria, enzymes catalyzing four of the reactions (glycosylase, AP endonuclease 1 (APE1), mitochondrial DNA polymerase Pol γ, and ligase III) have been identified; the enzyme that removes the AP site is one focus of this study.

Removal of the AP site is the rate-limiting reaction in BER.[2,3] As the DNA backbone is more solvent-exposed than the nucleobases, the deoxyribose moiety is more vulnerable to attack by highly reactive hydroxyl radicals, resulting in 20% of all dsDNA damage being found as oxidized deoxyribose.[4,5] In nuclear BER, the oxidation state of AP sites dictates the reaction pathways. A simple, unoxidized AP moiety enters the single-nucleotide base excision repair (SN-BER) subpathway, where the AP is removed by the dRP lyase activity of DNA polymerase β.[6] In contrast, oxidized deoxyribose, e.g., 2-deoxyribonolactone (dL),

halts SN-BER at the AP removal step owing to the formation of a covalent adduct with Pol β.[7] In this situation, repair enters the long-patch (LP) BER subpathway, where dL is removed by strand displacement DNA synthesis and cleavage of the displaced strand by flap endonuclease 1 (FEN1).[8] In SN-BER, only the lesion nucleotide is replaced, whereas in LP-BER, typically 2–12 nucleotides around the lesion site are replaced.

Although LP-BER products have been observed in human mitochondrial extract,[9–11] the nuclear LP-BER pathway does not appear to operate because the depletion of FEN1 does not affect mtDNA integrity.[12] Pol γ lacks strand displacement DNA synthesis ability and is only efficient in gap-filling synthesis when the gap size is greater than one nucleotide.[13] This observation suggests that Pol γ would be better suited for LP-BER than SN-BER if a larger DNA gap were created prior to gap-filling synthesis. Most importantly, however, no robust dRP lyase activity has been identified in mitochondria. Pol γ possesses only very low dRP lyase activity,[14] raising the question of whether it is adequate to remove extensive dRP lesions to maintain mtDNA integrity.

Human endo/exonuclease G (hEXOG) excises precisely two nucleotides from the 5′-end of DNA in a nicked or gapped DNA,[15,16] generating a minimum of a 2 nt DNA gap with a 3′-OH and a 5′-phosphate. This feature suggests that hEXOG could remove dRP and provide an optimal substrate for the subsequent BER reaction: Pol γ gap-filling synthesis. hEXOG is exclusively located in mitochondria; depletion of hEXOG elevates mtDNA single strand breaks but has no impact on nuclear DNA integrity and interrupts mtDNA repair prior to ligation.[12] hEXOG is found in complexes with other repair enzymes, e.g., APE1, Pol γ, and ligase III in mitochondrial lysates, and the quantity of the complex is increased under oxidative stress in cells.[17,18] This indicates that hEXOG is a component of the BER complex and its presence could also preclude the premature release of repair intermediates.[19]

We report here enzymatic and structural studies of the AP removal activity of hEXOG. We show that hEXOG possesses strong hydrolysis activity on a variety of AP substrates, including dRP, its oxidized adduct deoxyribonolactone (dL), and the stable analogue tetrahydrofuran (THF). Crystal structures of hEXOG complexed with AP-containing DNA reveal a mechanism for the enzyme's broad-spectrum activity. hEXOG also plays an important role in ensuring the correct order of subsequent BER reactions. Our studies therefore delineated the essential role of hEXOG in mitochondrial BER.

RESULTS

AP Removal by hEXOG.

AP hydrolysis activity by hEXOG was analyzed on a nicked dsDNA containing a 5′-AP that mimics the product of AP endonuclease I. The substrate consists of a 44 nt DNA annealed to an upstream 24 nt and a downstream 5′-^{32}P-AP-containing 20 nt DNA, where AP is dRP, THF, or dL (Figures 1 and 2 and Table S1). Both 5′-blunt ends of the DNA substrate are biotinylated to reduce irrelevant 5′-exonuclease activity. Removal of AP was monitored by the loss of radioactivity from the 5′-^{32}P-AP-DNA strand. Pol β and Pol γ were tested for comparison as Pol β has strong and Pol γ has weak dRP lyase activity. Reactions were carried out by incubating the DNA substrate with varying concentrations of hEXOG, Pol β,

or Pol γ. The excision product was quantified as the fraction of substrate reduction, defined as $(1 - [S]_E)/[S]_i$, where $[S]_E$ is the remaining substrate concentration at a given enzyme concentration [E] and $[S]_i$ is the initial substrate concentration.

By conducting reactions in the presence or absence of Mg^{2+}, the mechanism of AP removal can be assessed. Hydrolysis requires Mg^{2+} and releases a chemically unaltered dRP, while β-elimination occurs in the absence of Mg^{2+} and yields a 3′-α,β-unsaturated aldehydic derivative.[20] The β-elimination reaction forms a Schiff base intermediate between the ε-amine of a lysine residue in the enzyme and the C1′ of dRP.[21] Both dL and THF are unable to form a Schiff base and thus cannot be removed by β-elimination.[8,22]

5′-dRP Removal.—On the dRP-containing substrate, hEXOG, Pol β, and Pol γ all exhibit various levels of dRP removal activity (Figures 1a and S1). At 20 nM concentration of hEXOG, ~50% of maximal product was generated, slightly less than 68% of product generated by the same concentration of Pol β. However, only 18% was generated by Pol γ at 100 nM concentration. Using [product]/[enzyme] to normalize the data, hEXOG and Pol β, respectively, eliminated 14- and 18-fold more dRP from substrate DNA than Pol γ. The low dRP lyase activity of Pol γ is similar to that previously reported[14] and is not due to improper folding as the enzyme is fully active in primer extension (Figure S2). Although the catalytic efficiencies of hEXOG and Pol β are similar, their mechanisms are likely different, as the reported affinity of hEXOG to DNA is 35-fold higher, but the turnover rate is ~270-fold slower than Pol β.[16,23] Together these data suggest that hEXOG would preferentially bind to a dRP-DNA substrate if in direct competition with Pol β.

5′-THF Removal.—Pol β and Pol γ show negligible activity on THF-containing gapped DNA (Figure 1b), but hEXOG excised THF at an efficiency comparable to that on the dRP-containing substrate (Figure 1a,b). AP removal by hEXOG therefore utilizes a mechanism other than β-elimination. Comparable results were obtained using 3′-labeled substrates (Figure S3).

5′-dL Removal.—To make dL-containing DNA, we chemically synthesized 7-nitroindole (NI) phosphoramidite, a precursor of dL (Figures 2c and S4, Tables S3 and S4, and Supplementary Results). Immediately prior to use, NI-DNA was converted into dL-DNA by UV irradiation. As alkaline hydrolysis only affects UV-irradiated dL but not NI, conversion of ^{32}P-NI to dL was evaluated by quantifying the reduction of ^{32}P-NI upon UV treatment and alkaline hydrolysis. The conversion was near 100% (Figure 2a, lane 5). hEXOG effectively excises 5′-dL completely from the nicked dsDNA (Figure 2a,b).

Mechanism of hEXOG AP Lyase.

In the presence of $NaBH_4$, Pol β is covalently linked to the 5′-^{32}P-dRP-DNA substrate (Figure 3a, lanes 3 and 4), consistent with the β-elimination with a Schiff base intermediate.[24] No cross-linked product was detected with hEXOG (Figure 3a, lanes 1 and 2) despite the enzyme being fully active on the dRP-containing substrate (Figure 1a). In contrast to dRP removal by Pol β, that by hEXOG is completely dependent on the presence of Mg^{2+} (Figures 3b and S5a); furthermore, abolition of the catalytic histidine

(H140A) destroys the enzymatic activity (Figure S5b). These data confirm the conclusion that removal of AP by hEXOG is through hydrolysis, whereas Pol β uses β-elimination.

Structural Basis for Excision of AP by hEXOG.

Crystals of hEXOG complexed with dRP-DNA were formed with the nuclease-deficient H140A variant and a 5′-THF-10 nt DNA annealed to an 11 nt complementary strand (5′THF-10 nt/11 nt DNA, Figure 4c). The substrate mimics the downstream portion of a stable 5′-dRP-containing gapped DNA. Crystals of the hEXOG-5′THF-10 nt/11 nt complex belong to the $P2_12_12$ space group and diffract to 2.9 Å. The structure was determined by molecular replacement using a hEXOG-dsDNA complex[16] as a search model and refined to *R*-factor = 21.8% and *R*-free = 27.7% (Table S2).

The complex of hEXOG and 5′-THF-10 nt/11 nt DNA is a dimer. Each hEXOG monomer consists of a catalytic *Core* and a *Wing* domain; the dimer interface is formed by the N-terminal region of the *Core* domain and strengthened by domain swapping. The *Core* domain harbors the catalytic residue H^{140}. The 5′-THF-10 nt/11 nt dsDNA is bound in the cleft formed by the *Core* and *Wing* domains with the 5′-THF in the active site (Figure 4b).

As the structure contains the nuclease-deficient (H140A) variant, we derived an active hEXOG by replacing Ala^{140} with His from the wild-type hEXOG apo structure after superimposing the catalytic *Core* domain.[25] The RMSD of the superimposed backbone residues of the Core is 0.31 Å, lending confidence to the positioning of the docked histidine. For convenience, the DNA residues are numbered sequentially from the 5′-AP-containing substrate strand (Figure 4c). The base pair adjacent to the AP site, C_2–G_{10}, stacks against a platform formed by F^{307}, Y^{310}, and L^{311} (Figure 4f), which positions the nucleoside G_4 on the substrate strand 3.4 Å from H^{140}, thus poising H^{140} to catalyze a water-mediated strand breakage between the third phosphodiester bond from the 5′-end (Figure 4a,b). A Mg^{2+} ion is coordinated by three water molecules, N^{171}, a nonbridging oxygen, and the bridging oxygen of the scissile bond (Figure 4a,d), suggesting that hEXOG utilizes a divalent metal-dependent S_N2 reaction mechanism. The structure indicates that the product of hEXOG AP hydrolysis is a 5′-AP-2 nt, consistent with the solution results that hEXOG cleaved 5′-THF-19-Flsn and the product was 17-Flsn (Figure S3b).

The 5′-THF is frayed from the complementary strand (Figure 4e,f). The AP-binding site is distal to the catalytic site and forms electrostatic interactions with R^{314} and K^{148} at the 5′-phosphate (Figure 4a,e), suggesting that hEXOG AP hydrolysis should be unaffected by the chemical nature of the abasic site. This idea adequately explains the efficient cleavage by hEXOG of dRP-, dL-, and THF-containing DNA and likely other substrates.

To test this conclusion, we constructed a hEXOG C-terminal 68 aa deletion mutant (hEXOGΔC_{68}) that lacks the *Wing* domain and R^{314} as well as the residues that stabilize the substrate DNA for AP cleavage (F^{307}, Y^{310}, and L^{311}). hEXOG-ΔC_{68} showed significantly reduced dRP removal activity (Figure S5), confirming the structural conclusion that the *Wing* domain plays a critical role in substrate positioning and AP site recognition.

Structure of hEXOG Complexed with a Partial Gapped DNA.

To understand how hEXOG recognizes a gap in duplex DNA, we designed a gapped DNA of 24 nt annealed to 13 nt and 10 nt oligos at its 3′- and 5′-ends, respectively, and a 12/10 nt partial duplex DNA with 2 nt overhang at the 3′-end of the complementary strand that mimics the downstream portion of the gapped DNA for crystallization. Crystals containing gapped DNA diffracted to a resolution too low to be informative, but crystals of hEXOG complexed with the 12/10 nt DNA diffracted to 2.1 Å. The structure was determined using molecular replacement and refined to *R*/*R*-free to 0.202/0.238 (Table S2).

hEXOG binds the 10 bp duplex region of the 12/10 nt DNA in the same manner as a perfect duplex;[16] the single-stranded region of the complementary strand enters an opening between the *Wing* and *Core* domains, where both unpaired bases are flipped out relative to the duplex axis (Figure 5a,b). Helices from both the *Core* (K-helix) and *Wing* (O-helix) domains facilitate positioning of the unpaired single-stranded region with F^{307} and Y^{310} stacking with the blunt end of the partial DNA duplex. F^{258} is 4Å from the base moiety of G_{10} of the complementary strand, forming a sequence nonspecific interaction that guides the DNA away from the enzyme active site (Figure 5a).

The location of the single-stranded region of the complementary strand in the 12/10 nt DNA complex is similar to that in the hEXOG-THF-DNA complex structure (Figure 5b). We thus generated an hEXOG complex with AP-containing gapped DNA by docking a gapped DNA from the FEN1-DNA complex[26] onto the 12/10 nt DNA and THF-DNA complexes after superimposing the duplex regions (Figure 5c). The resulting two superimposed complementary strands are highly similar (RMSD = 1.9Å), lending confidence to the model. The composite AP-containing gapped DNA showed no steric clash with hEXOG, and the *Wing* domain is critical for bending the gapped DNA at a single-nucleotide gap or nick, thereby conferring the substrate specificity of hEXOG. The model also shows that the 5′-abasic site is frayed from the complementary strand by 16Å and sequestered within the active site of the enzyme. As hEXOG releases reaction products slowly, the structure further implies that hEXOG could prevent premature ligation of DNA prior to AP removal and gap-filling synthesis, thus ensuring the correct order of reactions in the BER pathway.

To test this hypothesis, we carried out ligation assays of THF-containing nicked DNA by human mitochondrial ligase III (Lig3) with and without hEXOG. In the absence of hEXOG, Lig3 ligates 5′-THF-containing DNA with similar efficiency to undamaged DNA (Figure S6). This abortive ligation was reduced by hEXOG in a concentration-dependent manner (Figure 5d). Ligation began to diminish at an hEXOG/Lig3 molar ratio of 2:1, suggesting that hEXOG can displace Lig3 from nicked DNA; hEXOG is thus capable of determining the reaction order of BER so that DNA endcleaning precedes Pol γ gap-filling synthesis, which is ultimately followed by ligation.

DISCUSSION

High levels of reactive oxygen species in mitochondria damage both nucleobase and deoxyribose moieties of mtDNA. In this study, we report that hEXOG performs the rate-limiting step of BER by processing 5′-abasic sites. The nuclear dRP lyase, Pol β, has

recently been reported to be present in mitochondria[27,28] despite no obvious mitochondrial localization sequence (MLS). This observation raises the question whether one or both enzymes function in mtBER. However, hEXOG acts on all AP sites irrespective of their chemical structures, whereas Pol β is specific for dRP and depletion of FEN1, which removes the flap in nuclear LP-BER and has no effect on AP removal in mitochondria (REF). Furthermore, while Pol β exists in all cell types,[29] its mitochondrial localization is cell type-specific: it is found in the brain and kidney but not in the liver, muscle, or heart.[30,31] In contrast, hEXOG is specifically localized to mitochondria in all cell types examined,[15] including those where Pol β is absent. These observations suggest that hEXOG is the primary enzyme used in mtBER, but its essential organismal function could possibly be complemented by Pol β in certain cell types.

A fundamental difference between EXOG and Pol β in dRP removal lies in the mechanism of reaction. EXOG employs a 5′-exonuclease activity, whereas Pol β uses β-elimination via a Schiff base intermediate.[24,21] This difference means that Pol β cannot remove oxidized dRPs, such as deoxyribonolactone dL, because it would covalently bond with a reaction intermediate. In contrast, hEXOG hydrolyzes the third phosphodiester bond from the 5′-abasic site; it is therefore expected to remove an AP site regardless of any chemical modification to the deoxyribose.

For efficient BER, enzymatic activities must be coordinated to ensure that the order of reactions is faithfully maintained. The order of BER could be ensured by the affinity of an enzyme for its specific repair intermediate. For example, the 5′-dRP-containing DNA is the substrate for the enzymes catalyzing dRP removal and ligation. This is particularly problematic in mitochondria as its only ligase, Lig3, catalyzes phosphodiester bond formation for abasic site-containing DNA almost equally well as intact DNA.[32] This premature ligation would regenerate the original abasic site without repair. It is therefore crucial to ensure that the Lig3 reaction follows dRP removal. Our current study shows that hEXOG effectively prevents premature ligation and, further, makes the subsequent BER reactions more efficient by generating the optimal gap for repair synthesis by Pol γ.

The division of nuclear BER into a single nucleotide and long patch is due to the lack of lyase activity in the nucleus for oxidized 5′-deoxyribose. The broad-spectrum activity of hEXOG suggests that mtBER can proceed with one pathway (Scheme 1). Our studies suggest that hEXOG plays multiple roles in mtBER by displaying a universal 5′-AP hydrolysis ability, generating an optimal product for the next reaction, and setting the reaction order. Our results augment additional evidence toward LP-BER being a major BER mechanism in mitochondria.

Supplementary Material

Refer to Web version on PubMed Central for supplementary material.

ACKNOWLEDGMENTS

The authors thank Ian Molineux for critical reading of the manuscript, Marc Greenberg for generous help with dL synthesis, and Christie Shumate for technical assistance. Coordinates of the hEXOG-DNA structures were deposited in the Protein Data Bank (PDB ID 7R6T and 7R6V).

Funding

The work was supported by a grant from NIH (GM110591 and AI134611 to Y.W.Y) and an endowment from the Smith and Sealy Foundation to the Sealy Center for Structural Biology. M.R.S. and A.K. were supported by the National Science Centre, Poland (Grant UMO-2016/21/P/NZ1/01085); this project has received funding from the European Union's Horizon 2020 Research and Innovation Programme under the Marie Skłodowska–Curie Grant Agreement No. 665778 as a part of a POLONEZ Fellowship.

ABBREVIATIONS

hEXOG	human exo/endonuclease G
Pol γ	DNA polymerase γ
Pol β	DNA polymerase β
BER	base excision repair
FEN1	flap endonuclease 1
mtDNA	mitochondrial DNA

REFERENCES

(1). Hudson EK; Hogue BA; Souza-Pinto NC; Croteau DL; Anson RM; Bohr VA; Hansford RG Age-associated change in mitochondrial DNA damage. Free Radical Res. 1998, 29, 573–579. [PubMed: 10098461]

(2). Srivastava DK; Berg BJ; Prasad R; Molina JT; Beard WA; Tomkinson AE; Wilson SH Mammalian abasic site base excision repair. Identification of the reaction sequence and ratedetermining steps. J. Biol. Chem 1998, 273, 21203–21209. [PubMed: 9694877]

(3). Wang Z; Wu X; Friedberg EC Molecular mechanism of base excision repair of uracil-containing DNA in yeast cell-free extracts. J. Biol. Chem 1997, 272, 24064–24071. [PubMed: 9295360]

(4). Breen AP; Murphy JA Reactions of oxyl radicals with DNA. Free Radical Biol. Med 1995, 18, 1033–1077. [PubMed: 7628729]

(5). Muftuoglu M; Mori MP; de Souza-Pinto NC Formation and repair of oxidative damage in the mitochondrial DNA. Mitochondrion 2014, 17, 164–181. [PubMed: 24704805]

(6). Allinson SL; Dianova II; Dianov GL DNA polymerase beta is the major dRP lyase involved in repair of oxidative base lesions in DNA by mammalian cell extracts. EMBO J. 2001, 20, 6919–6926. [PubMed: 11726527]

(7). Sung JS; Demple B Roles of base excision repair subpathways in correcting oxidized abasic sites in DNA. FEBS J. 2006, 273, 1620–1629. [PubMed: 16623699]

(8). Sung JS; DeMott MS; Demple B Long-patch base excision DNA repair of 2-deoxyribonolactone prevents the formation of DNA-protein cross-links with DNA polymerase beta. J. Biol. Chem 2005, 280, 39095–39103. [PubMed: 16188889]

(9). Akbari M; Visnes T; Krokan HE; Otterlei M Mitochondrial base excision repair of uracil and AP sites takes place by single-nucleotide insertion and long-patch DNA synthesis. DNA Repair 2008, 7, 605–616. [PubMed: 18295553]

(10). Liu P; Qian L; Sung JS; de Souza-Pinto NC; Zheng L; Bogenhagen DF; Bohr VA; Wilson DM 3rd; Shen B; Demple B Removal of oxidative DNA damage via FEN1-dependent long-patch

base excision repair in human cell mitochondria. Mol. Cell. Biol 2008, 28, 4975–4987. [PubMed: 18541666]

(11). Szczesny B; Tann AW; Longley MJ; Copeland WC; Mitra S Long patch base excision repair in mammalian mitochondrial genomes. J. Biol. Chem 2008, 283, 26349–26356. [PubMed: 18635552]

(12). Tann AW; Boldogh I; Meiss G; Qian W; Van Houten B; Mitra S; Szczesny B Apoptosis induced by persistent single-strand breaks in mitochondrial genome: critical role of EXOG (5′-EXO/endonuclease) in their repair. J. Biol. Chem 2011, 286, 31975–31983. [PubMed: 21768646]

(13). He Q; Shumate CK; White MA; Molineux IJ; Yin YW Exonuclease of human DNA polymerase gamma disengages its strand displacement function. Mitochondrion 2013, 13, 592–601. [PubMed: 23993955]

(14). Longley MJ; Prasad R; Srivastava DK; Wilson SH; Copeland WC Identification of 5′-deoxyribose phosphate lyase activity in human DNA polymerase gamma and its role in mitochondrial base excision repair in vitro. Proc. Natl. Acad. Sci. U.S.A 1998, 95, 12244–12248. [PubMed: 9770471]

(15). Cymerman IA; Chung I; Beckmann BM; Bujnicki JM; Meiss G EXOG, a novel paralog of Endonuclease G in higher eukaryotes. Nucleic Acids Res. 2008, 36, 1369–1379. [PubMed: 18187503]

(16). Szymanski MR; Yu W; Gmyrek AM; White MA; Molineux IJ; Lee JC; Yin YW A domain in human EXOG converts apoptotic endonuclease to DNA-repair exonuclease. Nat. Commun 2017, 8, No. 14959. [PubMed: 28466855]

(17). Szczesny B; Brunyanszki A; Olah G; Mitra S; Szabo C Opposing roles of mitochondrial and nuclear PARP1 in the regulation of mitochondrial and nuclear DNA integrity: implications for the regulation of mitochondrial function. Nucleic Acids Res. 2014, 42, 13161–13173. [PubMed: 25378300]

(18). Szczesny B; Marcatti M; Zatarain JR; Druzhyna N; Wiktorowicz JE; Nagy P; Hellmich MR; Szabo C Inhibition of hydrogen sulfide biosynthesis sensitizes lung adenocarcinoma to chemotherapeutic drugs by inhibiting mitochondrial DNA repair and suppressing cellular bioenergetics. Sci. Rep 2016, 6, No. 36125. [PubMed: 27808278]

(19). Wilson SH; Kunkel TA Passing the baton in base excision repair. Nat. Struct. Biol 2000, 7, 176–178. [PubMed: 10700268]

(20). Piersen CE; McCullough AK; Lloyd RS AP lyases and dRPases: commonality of mechanism. Mutat. Res 2000, 459, 43–53. [PubMed: 10677682]

(21). Prasad R; Batra VK; Yang XP; Krahn JM; Pedersen LC; Beard WA; Wilson SH Structural insight into the DNA polymerase beta deoxyribose phosphate lyase mechanism. DNA Repair 2005, 4, 1347–1357. [PubMed: 16172026]

(22). DeMott MS; Beyret E; Wong D; Bales BC; Hwang JT; Greenberg MM; Demple B Covalent trapping of human DNA polymerase beta by the oxidative DNA lesion 2-deoxyribonolactone. J. Biol. Chem 2002, 277, 7637–7640. [PubMed: 11805079]

(23). Prasad R; Beard WA; Strauss PR; Wilson SH Human DNA polymerase beta deoxyribose phosphate lyase. Substrate specificity and catalytic mechanism. J. Biol. Chem 1998, 273, 15263–15270. [PubMed: 9614142]

(24). Matsumoto Y; Kim K Excision of deoxyribose phosphate residues by DNA polymerase beta during DNA repair. Science 1995, 269, 699–702. [PubMed: 7624801]

(25). Dalton WS Targeting the mitochondria: an exciting new approach to myeloma therapy. Clin. Cancer Res 2002, 8, 3643–3645. [PubMed: 12473572]

(26). Tsutakawa SE; Classen S; Chapados BR; Arvai AS; Finger LD; Guenther G; Tomlinson CG; Thompson P; Sarker AH; Shen B; Cooper PK; Grasby JA; Tainer JA Human flap endonuclease structures, DNA double-base flipping, and a unified understanding of the FEN1 superfamily. Cell 2011, 145, 198–211. [PubMed: 21496641]

(27). Sykora P; Kanno S; Akbari M; Kulikowicz T; Baptiste BA; Leandro GS; Lu H; Tian J; May A; Becker KA; Croteau DL; Wilson DM 3rd; Sobol RW; Yasui A; Bohr VA DNA Polymerase Beta Participates in Mitochondrial DNA Repair. Mol. Cell. Biol 2017, 37, No. e00237-17. [PubMed: 28559431]

(28). Prasad R; Caglayan M; Dai DP; Nadalutti CA; Zhao ML; Gassman NR; Janoshazi AK; Stefanick DF; Horton JK; Krasich R; Longley MJ; Copeland WC; Griffith JD; Wilson SH DNA polymerase beta: A missing link of the base excision repair machinery in mammalian mitochondria. DNA Repair 2017, 60, 77–88. [PubMed: 29100041]

(29). Nowak R; Siedlecki JA; Kaczmarek L; Zmudzka BZ; Wilson SH Levels and size complexity of DNA polymerase beta mRNA in rat regenerating liver and other organs. Biochim. Biophys. Acta 1989, 1008, 203–207. [PubMed: 2736248]

(30). Kaufman BA; Van Houten B POLB: A new role of DNA polymerase beta in mitochondrial base excision repair. DNA Repair 2017, 60, A1–A5. [PubMed: 29129598]

(31). Hansen AB; Griner NB; Anderson JP; Kujoth GC; Prolla TA; Loeb LA; Glick E Mitochondrial DNA integrity is not dependent on DNA polymerase-beta activity. DNA Repair 2006, 5, 71–79. [PubMed: 16165404]

(32). Simsek D; Furda A; Gao Y; Artus J; Brunet E; Hadjantonakis AK; Van Houten B; Shuman S; McKinnon PJ; Jasin M Crucial role for DNA ligase III in mitochondria but not in Xrcc1-dependent repair. Nature 2011, 471, 245–248. [PubMed: 21390132]

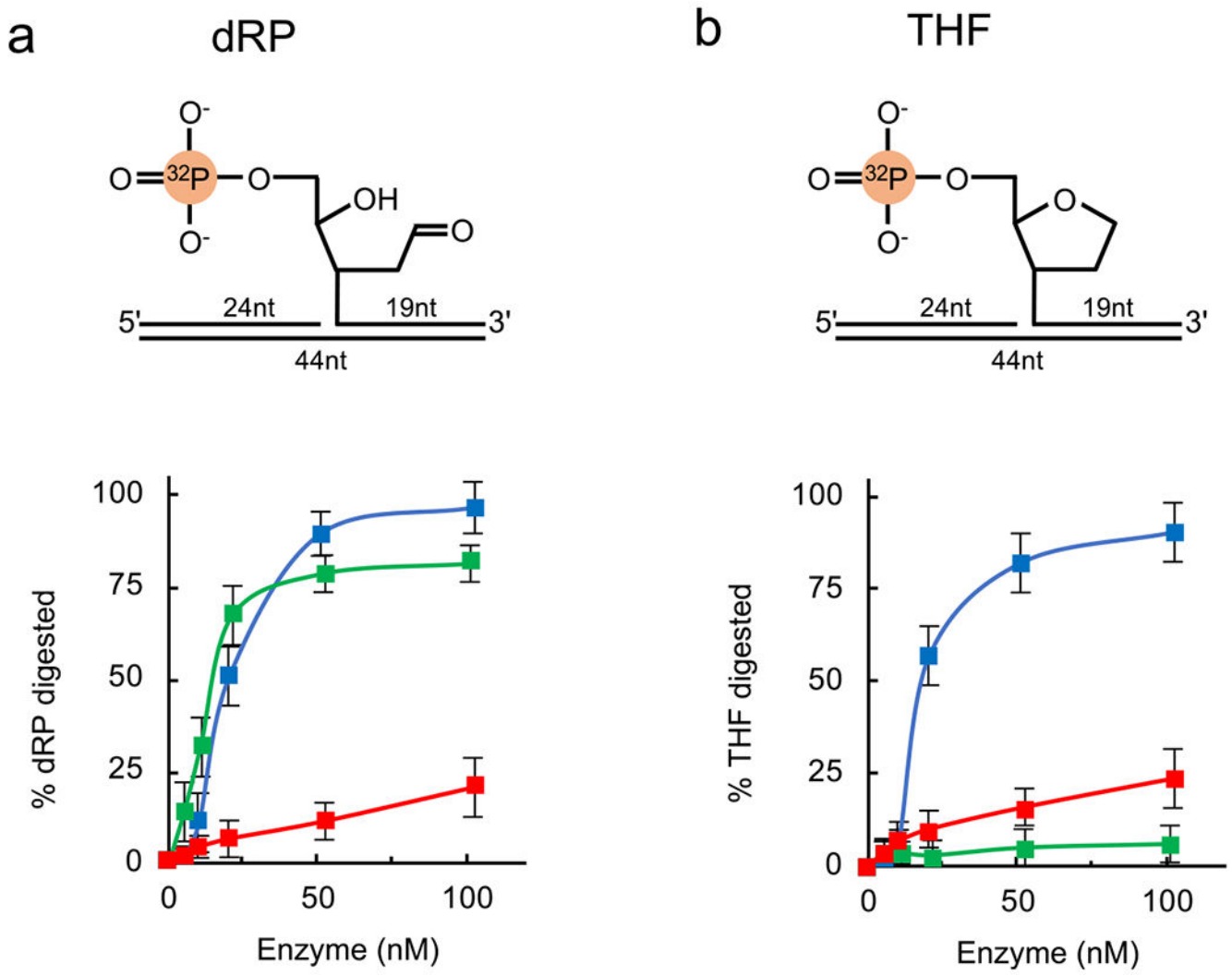

Figure 1.

AP removal activity of hEXOG, Pol β, and Pol γ. Activities of hEXOG (blue), Pol β (green), and Pol γ (red) on digestion of 5′-^{32}P-labeled DNA dRP (a) or THF (b). For clarity, the biotin blockers on the DNA ends are not shown. The graphs represent the mean values with standard deviations (error bars) from three experiments. Reactions were carried out for 5 min at 37 °C using 5 nM DNA substrate and hEXOG, Pol β, or Pol γ in the presence of 10 mM $MgCl_2$.The raw data are presented in Figure S1.

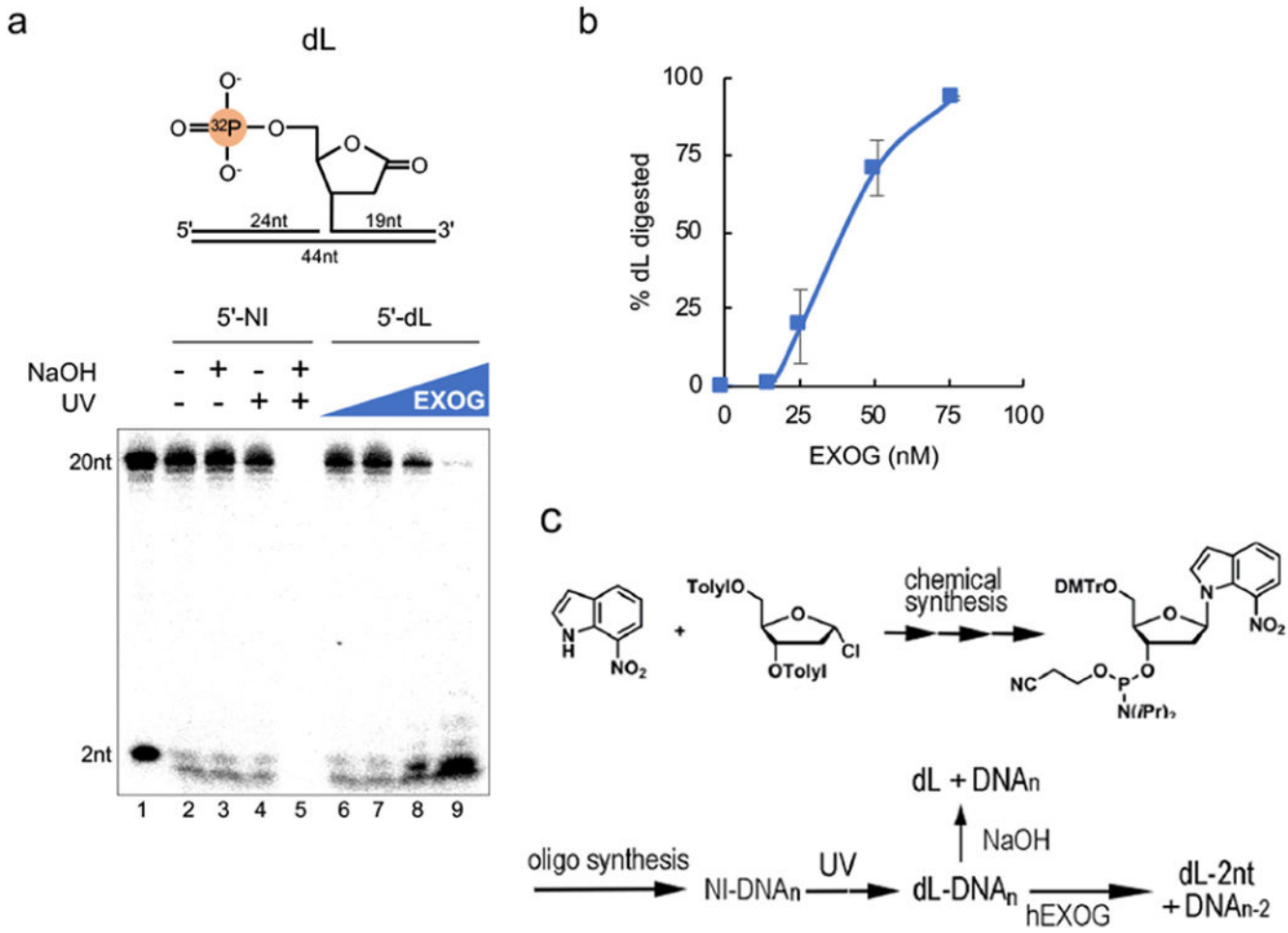

Figure 2.

hEXOG cleavage of the oxidized abasic site dL. (a) Conversion of nitroindole (NI)-containing DNA to deoxyribonolactone (dL) and the hydrolysis activity of hEXOG on dL-containing DNA. Lane 1: molecular weight standard, lane 2: NI-DNA, lane 3: NaOH-treated NI-DNA, lane 4: UV-treated NI-DNA, lane 5: UV- and then NaOH-treated NI-DNA, lanes 6–9: dL-containing DNA (10 nM) processed by hEXOG for 5 min at 37 °C in the presence of 10 mM $MgCl_2$. (b) Quantification of the data in panel (a). The graph presents the mean values with deviations (error bars) from two experiments. (c) Schematic of dL-containing DNA synthesis.

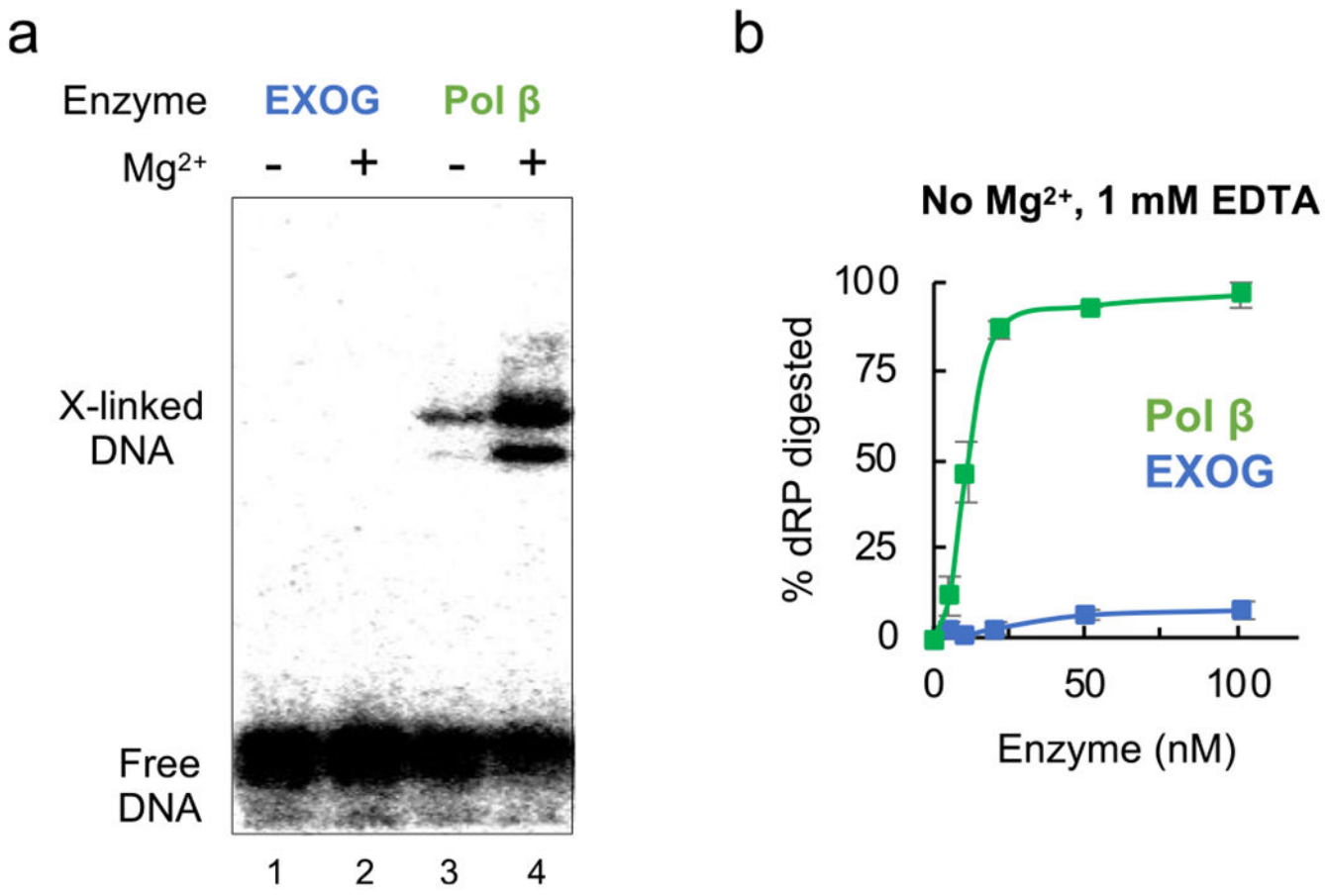

Figure 3.

dRP removal by hEXOG and Pol *β*. (a) hEXOG (51 nM) or Pol *β* (58 nM) incubated at 0 °C with 10 mM 5′-^{32}P-dRP-containing DNA and 20 mM $NaBH_4$ with or without 10 mM $MgCl_2$. (b) Quantification of enzyme concentration-dependent dRP removal (raw data are shown in Figure S4).

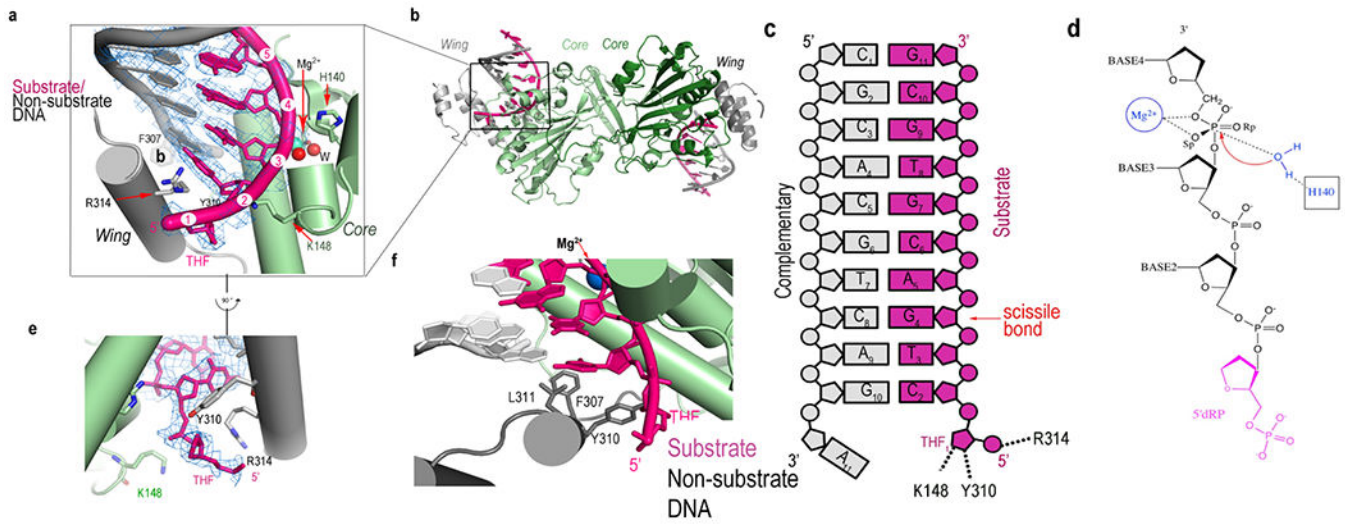

Figure 4.

Crystal structures of hEXOG H140A. (a) Active site of hEXOG shows the scissile bond at the third phosphodiester bond, yielding a 5′-THF-2 nt product. The catalytic H^{140} is docked from the Apo hEXOG structure after superposition of the Core domains. The electron density of THF-10 nt/11 nt DNA is shown in the blue mesh. F^{307} contributes to the tape-measured cleavage. 5′-THF is stabilized by R^{314}, K^{148}, and Y^{310} from the Wing domain. (b) Overall structure showing the homodimer hEXOG; each monomer contains a catalytic Core domain (green) and a Wing domain (gray). The DNA contains a 5′-THF-10 nt substrate (magenta) and an 11 nt complementary strand (gray). (c) Scheme of the DNA substrate. (d) Proposed nucleolytic reaction mechanism of hEXOG. (e) Interaction of THF with hEXOG. (f) Terminal base pair interaction with F307, Y310, and L311.

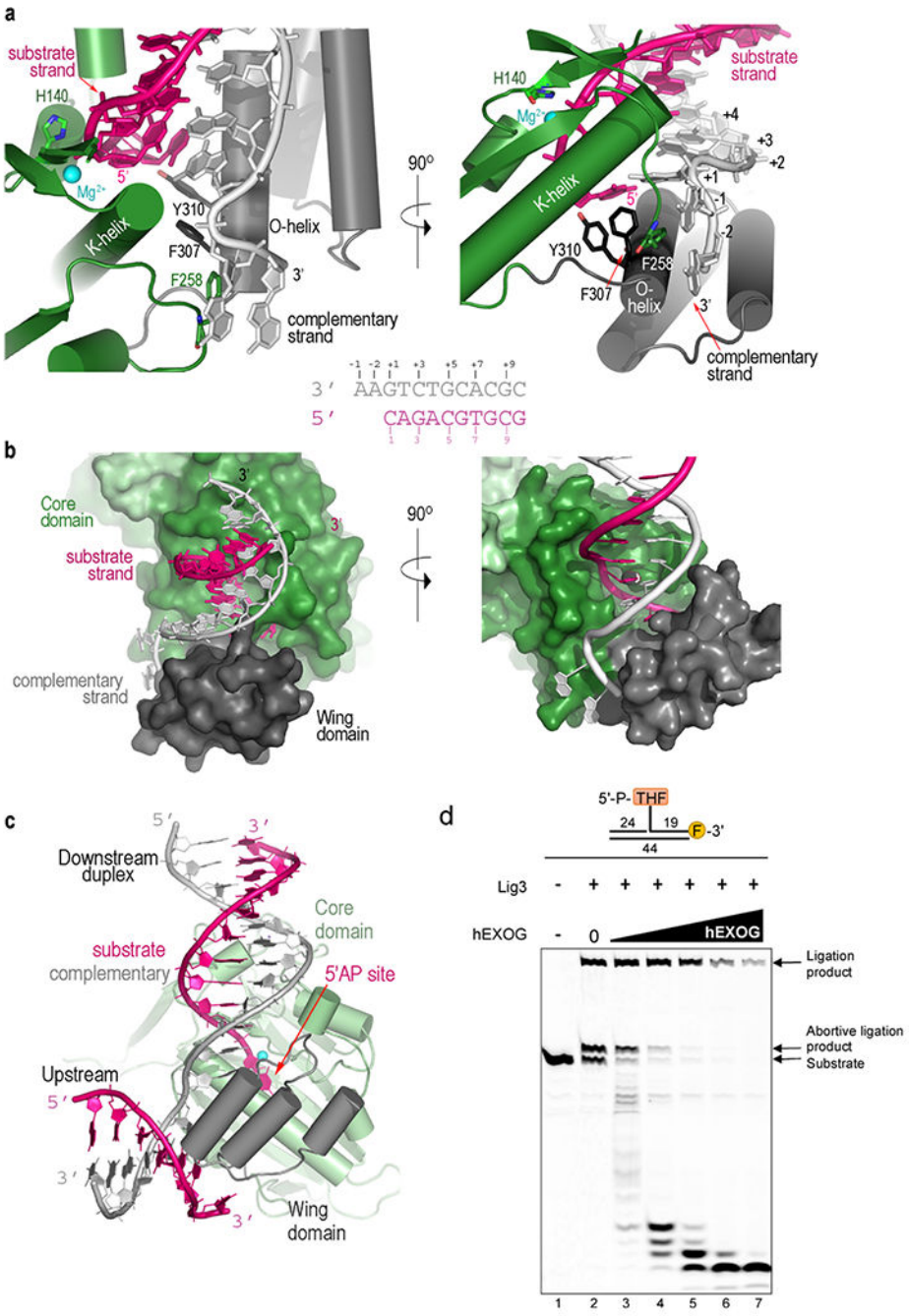

Figure 5.

Crystal structure of a partially gapped DNA and the effect of hEXOG on the order of BER reactions. (a) Active site of 10/12 nt partial duplex showing the strand separation by K-helix of the Core domain and Y^{310} and F^{307} of the Wing domain. The −1 and −2 residues of the complementary strand are flipped out by ~90°. The DNA sequence in the crystal is shown. (b) Surface rendition illustrating that the 3′-end of the complementary strand departs from the 5′-end of the substrate strand. (c) Modeling indicates that the 5′-end of the substrate strand is protected by hEXOG. (d) Ligation of the THF-containing substrate (50 nM) in

the presence of Lig3 (50 nM) and increasing concentrations (10, 25, 50, 100, 200 nM) of hEXOG. Reactions were carried out for 5 min at 37 °C in the presence of 10 mM $MgCl_2$ and 1 mM ATP. A representative image from three independent experiments is shown.

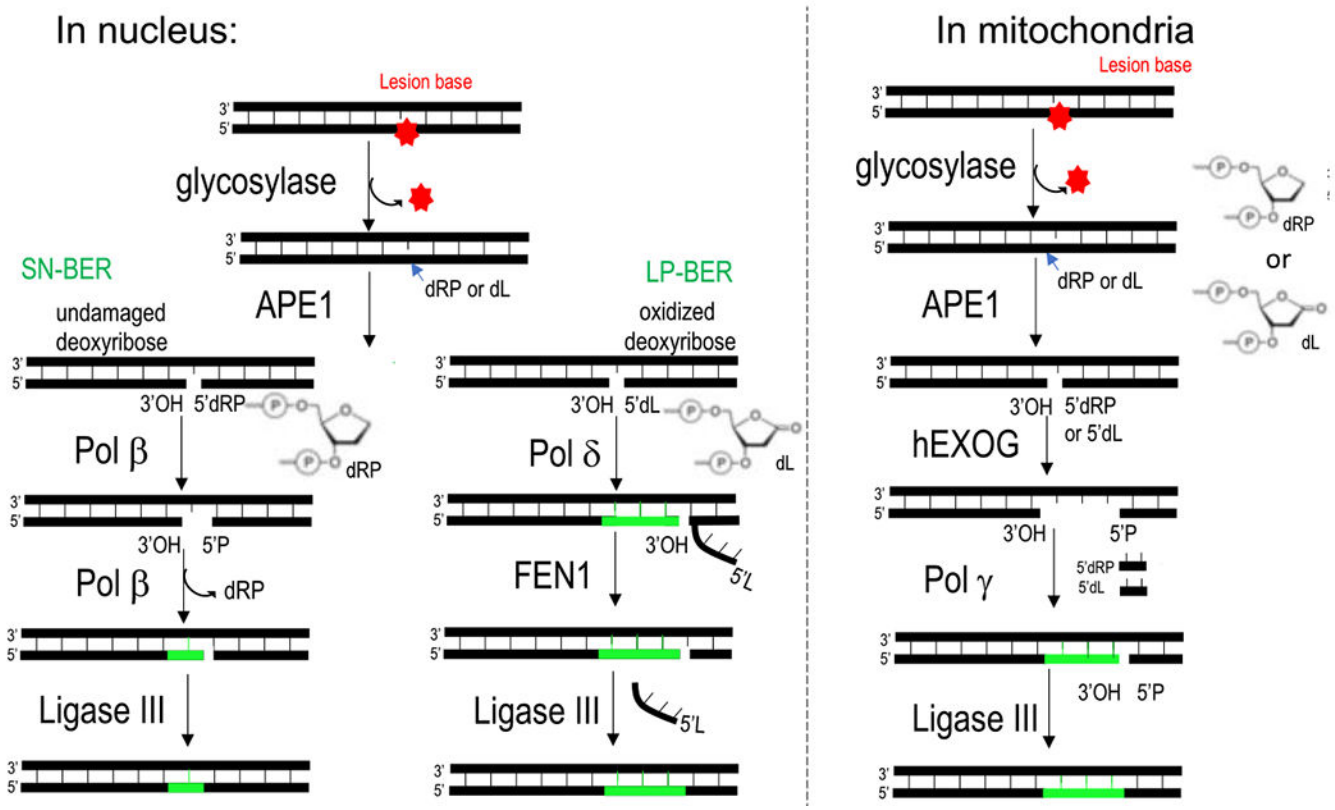

Scheme 1. BER in Nucleus and in Mitochondria[a]

[a]The nuclear BER is based on existing literature, and the mitochondrial pathway is proposed based on this study.